Applied Water Science (2025) 15:101
https://doi.org/10.1007/s13201-025-02453-x

ORIGINAL ARTICLE

Degradation of bacteria for water purification in a TiO2-coated photocatalytic reactor illuminated by solar light

Lukas Dufner[1,3] · **Philipp Hofmann**[1,3] · **Daniel Dobslaw**[2,3] · **Frank Kern**[1,3]

Received: 19 March 2024 / Accepted: 21 March 2025 / Published online: 18 April 2025

Abstract

In this study, the inactivation of various bacterial strains in a solar illuminated photocatalysis reactor with a titania photocatalyst dispersed in a geopolymer coating is studied. The modular reactor design consists of connected catalyst-coated open water carrying chutes. The cleaning efficiency of the process against chemical and biological water contaminants was evaluated by means of test series with methylene blue as a reference for chemical contamination and by studying the inactivation of the strains *Escherichia coli, Bacillus subtilis, Pseudomonas fluorescens* and an undefined mixed culture from the effluent of the secondary clarifier of a wastewater treatment plant as biological contaminants. Test series with methylene blue showed reduction efficiencies of 17–63% for non-catalyst-coated reference reactors and 55–99% for catalyst-coated reactors within 120–300 min of exposure to natural sunlight. Disinfection test series showed reduction efficiencies of 0.0–2.8 log units (without catalyst) and 0.0–4.4 log units (with catalyst) for mentioned bacteria and the mixed culture within 40–180 min of light exposure. Hence, the catalyst-coated system consistently showed a significantly higher degradation efficiency than the non-coated reference. A comparison of methylene blue degradation under natural solar irradiation and artificial UVA irradiation conditions showed that this simple reactor concept is suitable for the combined elimination of trace substances and disinfection of water even at moderate flux rates of 1000 W/m^2.

Keywords Photocatalysis · Disinfection · TiO_2 · Solar reactor · Bacteria degradation

Introduction

According to the World Health Organization (WHO), at least 1.7 billion people, mainly in water stressed countries, are forced to use fecally and therefore microbially contaminated drinking water. The consumption of these contaminated water sources enforces transmission of waterborne diseases such as diarrhea, cholera, dysentery, typhoid and polio, leading to approximately 505,000 deaths worldwide per year (WHO 2022a; Dungumaro 2007). Therefore, it is not surprising that UNICEF documented poor hygiene, inadequate sanitation and unsafe water as reasons for about 90 percent of the global diarrhea deaths (UNICEF 2012). Furthermore, diarrheal diseases are responsible for 4.1% of the total disability-adjusted life year (DALY) global burden of disease and caused average total costs of $52 for outpatient and $216 for impatient care in 137 low- and middle-income countries in 2015 (Baral et al. 2020). The economic costs of diarrheal diseases might amount nearly 4% of the GNP of these countries (Hasan et al. 2021). In 2022, only around 73% of the world´s population (5.8 billion people) had access to hygienically safe drinking water resources that might be used without restrictions (WHO 2022b). Humans with access to unsafe water resources, however, commonly suffer from poverty, as water-related diseases cause losses in productive working hours, increased health costs and negatively impact food security (Adelodun et al. 2021), human development indicators (Rahut et al. 2015), fertility and migration trends (Falkenmark 1990).

To face stated problems, the United Nations created the sustainable development goals to be reached in 2030, where No. 6 focuses on clean water and sanitation to ensure

✉ Lukas Dufner
Lukas.dufner@ifkb.uni-stuttgart.de

1 Institute for Manufacturing Technologies of Ceramic Components and Composites, University of Stuttgart, 70569 Stuttgart, Germany

2 Institute of Spatial and Regional Planning, University of Stuttgart, 70569 Stuttgart, Germany

3 TTI Technology Transfer Initiative GmbH of the University of Stuttgart, ALR-Umwelt TGU, 70569 Stuttgart, Germany

the availability and sustainable management of water and sanitation for all (United Nations 2015). Although central treatment of drinking water and its supply via water networks is effective in densely populated regions, far-flung communities, rural areas with poor infrastructure and rural areas in developing countries in general require decentralized solutions. Therefore, household water treatment (HWT) solutions are being promoted and needed to prevent harmful diseases (Hunter 2009; Loeb et al. 2016). However, many current solutions are inefficient or associated with high energy consumption (WHO 2017). To overcome these problems, a solar batch-process disinfection method (SODIS) has been developed, which has proven to be an effective treatment for microbially contaminated water. SODIS works with water-filled transparent plastic or glass bottles exposed to sun radiation for at least 6 h on a sunny day (McGuigan et al. 2012) to kill effectively pathogenics like bacteria, phages, viruses, fungal spores and protozoa (Masjoudi et al. 2021; Hijnen and Medema 2005; Hijnen 2009b). UV-B light (280–320 nm) absorption is one of the main UV-induced disinfection mechanisms as light is absorbed by the double bonds of the pyrimidine bases in the DNA strand causing dimerization of adjacent pyrimidine bases (Cleaver 1974; Kuzminov 2013; Banaś et al. 2020). However, various microorganisms reveal photolyase activity turning around dimerization after light uptake—a repair mechanism well-known as photoreactivation (Cleaver 1974; Li et al. 2017; Quek et al. 2008). Beside naturally high UV tolerance or resistance according to cell wall structures like in gram-positive cells or endospores, repair mechanisms as described cause treatment ineffectivity. Hence, some microorganisms cannot be treated by SODIS alone and require further treatment efforts. An enhanced SODIS approach boosted with photocatalyst, which can also kill UV-resistant microorganisms through sunlight-induced oxidative processes, appears suitable for this purpose (Dionysiou et al. 2016).

Disinfection performance strongly depends on physical-chemical and biological parameters as mentioned before. All bacteria (both vegetative cells and endospores) and viruses relevant to drinking water originate from fecal contamination. While viruses in particular can survive for several months in aquifers due to temperature and UV shielding (Botzenhart 2007), vegetative bacterial cells in particular are much more susceptible to UV radiation (Hijnen 2009b; Hijnen and Medema 2005) than viruses. Nevertheless, bacterial indicators have become established because they are easier to cultivate and detect. For example, *Escherichia coli* (E. coli) is used as a general fecal indicator (Bundesministerium für Gesundheit 2001; García-Gil et al. 2021); the endospore-forming *Bacillus subtilis* can be used as a particularly UV-resistant microorganism (Guimarães and Barretto 2003; Gutiérrez-Alfaro et al. 2016; Lonnen et al. 2005) and *Pseudomonas fluorescens* may be used as a non-pathogenic surrogate of *Pseudomonas aeruginosa* representing antibiotic-resistant or generally human-pathogenic germs (Chen et al. 2010; Dunlop et al. 2010; Lonnen et al. 2005). Due to their different physiology (including the structure of the cell wall and Gram behavior), physiological state, strain variations, the occurrence of different protective and repair mechanisms against oxidative stress (Deng et al. 2020) and the form of cultivation (i.e., single cell, flocs, biofilm) (Hijnen 2009a), there is a wide variation in the detected disinfection performance (Gutiérrez-Alfaro et al. 2016; Lonnen et al. 2005).

Photocatalysis by semiconductors like titanium dioxide (TiO_2) belongs to the advanced oxidation processes (AOPs) and is a promising process for mineralization of organic materials like bacteria, viruses and micropollutants to CO_2 and H_2O (Pichat 2013; Dionysiou et al. 2016). The degradation is based on highly reactive hydroxyl radicals exerting a nonselective oxidation of organic matter. The efficiency of titania photocatalyst in various field such as degradation of metallic or other inorganic pollutants, disinfection of water, purification of air and generation of hydrogen is well documented in the literature (Ismael 2020; Omar et al. 2020; Ochiai and Fujishima 2012). Titanium dioxide (TiO_2) offers high activity combined with biocompatibility, low cost, non-toxicity and photostability (Dionysiou et al. 2016; Pichat 2013; Schneider et al. 2016). Activity of titania is mainly governed by phase composition, with the thermodynamically instable anatase phase showing superior activity to thermodynamically stable rutile (Bojinova et al. 2007). The mixed anatase/rutile TiO_2 powder P25 manufactured by Evonik AG has a proven track record as an active photocatalyst and is considered as benchmark in terms of activity (Ide et al. 2016). The required excitation frequency depends on the bandgap of the semiconductor, which—in case of anatase phase TiO_2—is 3.3 eV. This corresponds to a wavelength less than 375 nm, equivalent to the UVA range of the light spectra. Focusing on solar light instead of expensive artificial UVA light for catalytic activation reveals a considerable potential in saving of resources and improving treatment performance (Koltsakidou et al. 2017; Fouad et al. 2021; Dionysiou et al. 2016; McGuigan et al. 2012; Schneider et al. 2016; Fox and Dulay 1993; Shannon et al. 2008; Malato et al. 2009). Sufficient illumination can be expected within the sunbelt region (+/− 35° of latitude respect to the equator), where the highest irradiation fluences are observed (Moreno-SanSegundo et al. 2021). It should be noted that only a small part of the solar irradiation is in the UVA range and able to trigger photocatalysis in anatase phase TiO_2. Various reactor concepts of enhanced SODIS in combination with a photocatalyst were previously shown (Dionysiou et al. 2016; Alrousan et al. 2012; Khan et al. 2012; Oelgemöller et al. 2006). However, they require either

expensive materials and complicated technology, or exhibit high cost for maintenance and/or electrical energy.

This study focuses on a low-tech approach using materials readily available, 3D-printed parts and a simple coating process for a sufficient photocatalytic water treatment solely powered by solar energy.

Materials and methods

Preparation of TiO_2 catalyst coatings

The exact preparation procedure of the coatings was previously described elsewhere (Dufner et al. 2023). Briefly, 10 g potassium silicate solution consisting of modified aluminosilicate and modified alkali silicates (Geosil14517, Woellner GmbH, Ludwigshafen, Germany), also known as"water glass,"was premixed with 12.5 g of hardener (Stabisil 40, Woellner GmbH, Ludwigshafen, Germany). Subsequently 1 g of TiO_2 powder (P25—Evonik AG, Essen, Germany) and 2 g of H_2O were added, and the mixture was stirred for 10 min. This ready-to-use suspension was applied directly to the polished aluminum substrate by a simple rolling process and cured for 24 h at room temperature. Then, a second layer of coating is applied by the identical procedure to reach a total coating thickness of approximately 100 µm.

Reactor concept

The reactor concept follows a modular system of water carrying aluminum U-profiles (650 mm length, 60 mm width and 15 mm height) and 3D filament-printed polymer connector elements, and a 3D-printed water inlet and outlet. A reactor, consisting of 2 aluminum profiles, one connecting element, and one inlet and outlet each, represents the smallest possible concept design, which was already presented elsewhere (Dufner et al. 2024). For experiments in the laboratory under artificial UVA radiation, this small 2-level reactor (R2) was installed. Carrying out experiments under solar radiation, a scaled-up reactor with 18 levels (R18) at a footprint of a Euro pallet (1200 mm × 800 mm) was installed on a wooden support (see Fig. 1). A second reactor with the same geometry but without catalytical coating was installed as reference in both cases. The reactors parameters are shown in Table 1.

Experimental setup

Both reactor systems R2 and R18 were operated differently. For every test with the R2 or R18 photocatalyst-coated reactor under solar irradiation, an identical but uncoated reactor was used as reference, installed directly next to the coated one and operated simultaneously under the same conditions

Fig. 1 Uncoated 18-profile reactor with the numbered profiles from which the samples are taken

Table 1 Reactor properties

Reactor properties	2-profile reactor (R2)	18-profile reactor (R18)
Aluminum profiles [–]	2	18
Connecting elements [–]	1	17
Inlet [–]	1	1
Outlet [–]	1	1
Volume [dm^3]	0.62	5.6
Catalyst area [dm^2]	7.8	70.2
Height difference delta H [cm]	1.6	28.8
Structure	Printed (PLA)	Wood

to quantify photocatalytic performance and to differentiate it from the arising UV disinfection. After initial tests of R2 under artificial conditions, consecutive tests of R2 and R18 were performed outside on sunny days according to Table 2 (solar radiation measurement see chapter 2.4). Test time was varied from 180 min under solar irradiation to 300 min under UVA radiation in the laboratory.

Reactor operation R2

R2 was operated as a loop reactor with either a bacterial suspension or an aqueous methylene blue solution at a total volume of 1 L. The reactor effluent was collected in a storage tank and recirculated via a peristaltic pump to the reactor inlet (see Fig. 2) at a flow rate of 40 mL min^{-1}. For artificial UVA radiation, two 15 W UVA lamps with a wavelength of 365 nm (VL-215.BL, Vilber, France, total power 30 W) were mounted 100 mm above the profile bottom level. To reach the adsorption equilibrium, the solution was initially circulated for 15 min without illumination, afterward repetitive 30

Table 2 Overview of experiments

Experiment	Reactor	Light source	Degradation substance/bacteria
R2_UVA_MB	R2	Artificial UVA	Methylene blue
R2_SUN_MB1	R2	Solar light	Methylene blue
R2_SUN_MB2	R2	Solar light	Methylene blue
R2_SUN_MB3*	R2	Solar light	Methylene blue
R2_SUN_Ecoli**	R2	Solar light	*Escherichia coli*
R18_SUN_MB	R18	Solar light	Methylene blue
R18_SUN_Ecoli*	R18	Solar light	*Escherichia coli*
R18_SUN_BaSu*	R18	Solar light	Bacillus subtilis
R18_SUN_PsFl*	R18	Solar light	Pseudomonas fluorescens
R18_SUN_Mix*	R18	Solar light	Mixed bacteria culture

*A control test without catalyst coating was carried out for this test, too

**Supplementary information

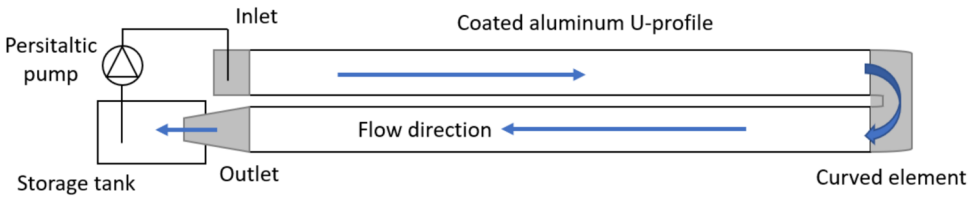

Fig. 2 Operation mode for R2 reactor (bird's eye view)

min sampling started. The 2-ml samples were taken from the storage tank, as the concentration there is homogeneous due to the mixing, the degree of decolorization was determined and then returned.

Reactor operation R18

Similar to R2 conditions, the R18 experiments were also carried out under batch conditions. Due to the high residence time of the test solution in the reactor, the experiment was operated as a pass-through reactor. In detail, either 10 L of saline solution (for preparation see chapter 2.4.) contaminated with bacteria or methylene blue solution were prepared for each reactor and covered by a lid as protection against UV light (see Fig. 3). The solutions were placed in the storage tank and continuously mixed by a magnetic stirrer (300 rpm) to prevent sedimentation of bacteria. The suspensions were pumped by a peristaltic pump at a flow rate of 40 mL min^{-1} to the inlets of the respective reactors. After a residence time of around 120 min, the fluid passed the end of the reactor and was collected in a separate tank. When the test medium emerged, sampling was initially carried out after 30 min and repeated in 30-min intervals at each outlet of the profiles No. 1, 3, 6, 12 and 18 collecting sample volumes of 2 ml. Quantification of bacterial concentrations was performed according to the description below. Water temperature was measured immediately before sampling to exclude thermal disinfection co-effects at each sampling position.

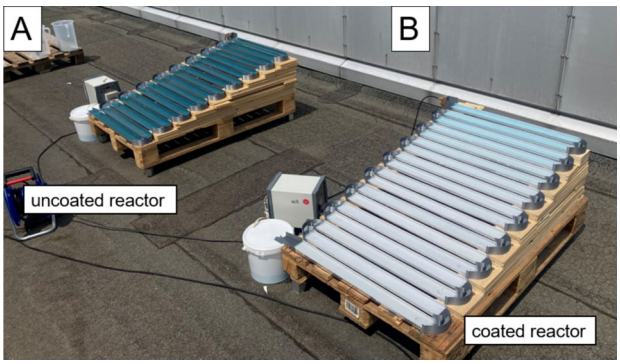

Fig. 3 Experimental setup: R18 coated reactor (**B**) and uncoated reactor (**A**) during methylene blue degradation experiment

Measurement of solar radiation

The test site was located on the Campus Vaihingen of the University of Stuttgart (latitude 48° 44´ N, longitude 9° 05´ E), Germany. The experiments were carried out in natural solar light in the time frame of 10 am to 4 pm to utilize the highest daily solar radiation dose. Water temperatures during test runs reached maximum 33 °C and were not detrimental to the vitality of germs or chemical auto degradation. Solar radiation data were provided by the meteorological station Lauchäcker, Stuttgart, located in a distance of 560 m from the test site. The solar radiation was measured by the CNR1 Net Radiometer (Kipp and Zonen, Delft, The Netherlands) in the range from 305 to 2800 nm.

Chemicals and microbial strains

The photocatalytically induced degradation rate of chemical pollutants was monitored observing decolorization of a methylene blue solution at a concentration level of 10 µmoL × L^{-1}. The microbiological activity was evaluated using the environmental relevant bacteria *Escherichia coli* B DSM 613 (gram-negative strain), *Bacillus subtilis* DSM 10 (gram-positive strain), *Pseudomonas fluorescens* DSM 50090 (gram-negative strain) and a bacterial mixed culture isolated from the effluent of the secondary settling tank of the WWTP Stuttgart-Büsnau. Methylene blue and all chemicals used for cultivation were of pro analysis quality.

Microbial cultivation and sampling

Cultivation was initiated by spreading aliquots of the frozen cultures of all three bacterial strains onto LB agar plates and initial cultivation for one week at 30 °C. Subsequent strain management was carried out by striking out single grown colonies onto fresh media twice a week. In preparation of the test series, colonies were taken from an overnight media plate, transferred to fresh media plates, again incubated overnight at 30 °C and transferred into flasks with sterile 50 mL LB-Miller medium and cultivated overnight in a rotary shaker at 121 rpm and 30 °C. Overnight grown cultures were each added to 10 L of 0.9% saline, resulted in a final cell density of around 10^6 CFU × mL^{-1}. Due to the high dilution factor of 1:200, no prewashing of the grown cultures was carried out. Samples of WWTP effluent were freshly collected and immediately cooled down to 4 °C for transport to the test site. During photocatalytical test series, samples were immediately cooled down to 4 °C, and the set of samples was further processed within 3 h. Serial dilutions of the samples using saline were prepared and plated onto LB agar via drop plate method (Herigstad et al. 2001; Hoben and Somasegaran 1982; Reed and Reed 1948). After overnight incubation at 30 °C, dilutions with 3–30 visible colonies were selected for enumeration. Bacterial concentrations were calculated according to the dilution used for counting regarding DIN EN ISO 8199.

Characterization of photocatalyst activity

The photocatalytic activity against chemical contaminants was quantified by the grade of decolorization, and therefore, photodegradation of a methylene blue solution with 10 µmol × L^{-1} concentration against time, which can be measured best at the characteristic peak in the absorption spectra of methylene blue at 664 nm (Svoboda et al. 2020). In this work, each sample was analyzed by a UV–VIS spectrometer (Specord 210 Plus of Analytik Jena) to measure the absorption spectra. Afterward, the sample was returned to the main solution. As methylene blue shows anionic tensidic characteristics (DIN EN 903 1994), a group of contaminants mainly present in industrial wastewater like effluents of textile industries, and it is commonly used to examine photocatalytic degradation in a couple of studies (Rauf et al. 2010; Vasiljevic et al. 2020; Xia et al. 2015).

For quantification of microbial disinfection efficacy of the process, samples were taken after 0, 40, 80 and 120 min (*Bacillus subtilis, Escherichia coli*) and additional 20 min (only *Pseudomonas fluorescens* and mixed culture). Samples were further processed and quantified according to the procedure described above.

Results and discussion

Effect of light intensity

Impact of solar light intensity on the degradation of methylene blue as a reference compound for chemical contamination was initially investigated in the small R2 test setup, whereby the four test series R2_UVA_MB, R2_SUN_MB1, R2_SUN_MB2 and R2_SUN_MB3 were carried out. While the R2_UVA_MB series was done under artificial laboratory conditions and thus a defined UVA light exposure (385 W/m^2), the series R2_SUN_MB1, R2_SUN_MB2 and R2_SUN_MB3 represent real measurements under varying light and UVA intensities in the range of 250–1200 W/m^2, i.e., 88% of the earth´s average value (so-called solar constant; 1361 W/m^2) (International Astronomical Union 2015) was achieved in peak. The average for the region of Stuttgart is around 1000 W/m^2 on a blue-sky-sunny-day which is compared to the regions within the sunbelt, very low (Moreno-SanSegundo et al. 2021; Landesanstalt für Umwelt Baden-Württemberg 2024). The results are shown in Figs. 4 and 5 (outdoor tests, except R2_SUN_MB3) and 6 (indoor tests) (Fig. 6).

Both runs shown in Fig. 4 (sunny day) and Fig. 5 (cloudy to sunny day) showed an exponential decay curve for the decolorization of methylene blue, i.e., in absorbance at 664 nm. The exponential decay behavior in both runs followed first-order reaction kinetics even at cloudy conditions (during time periods of 60–90 min at approx. 110 min and 120–140 min), even though a significant drop in the light intensity and thus in decolorization kinetics was expected. In fact, there was no noticeable difference in the two progress curves, as the residual concentration in both series fell to approx. 50%, 30%, 20%, 13%, 8% and 4% after 40, 60, 90, 120, 150 and 180 min, respectively. The continued decolorization of the methylene blue, which was also observed during the pronounced cloudy phase, indicates the relevance of photons outside the UVA spectrum.

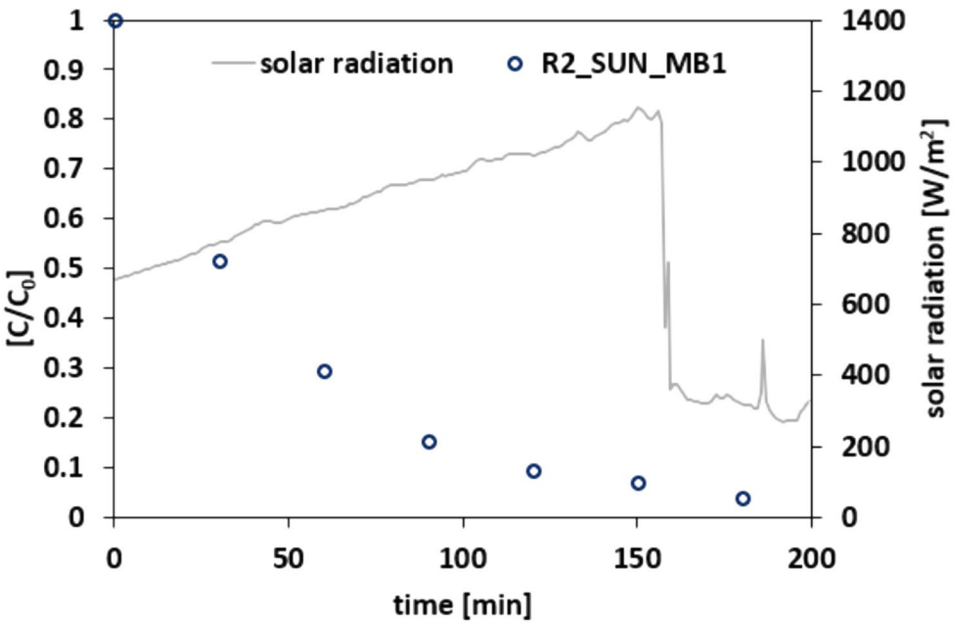

Fig. 4 Degradation of methylene blue over time under solar radiation for test R2_SUN_MB1 in the 2-profile reactor

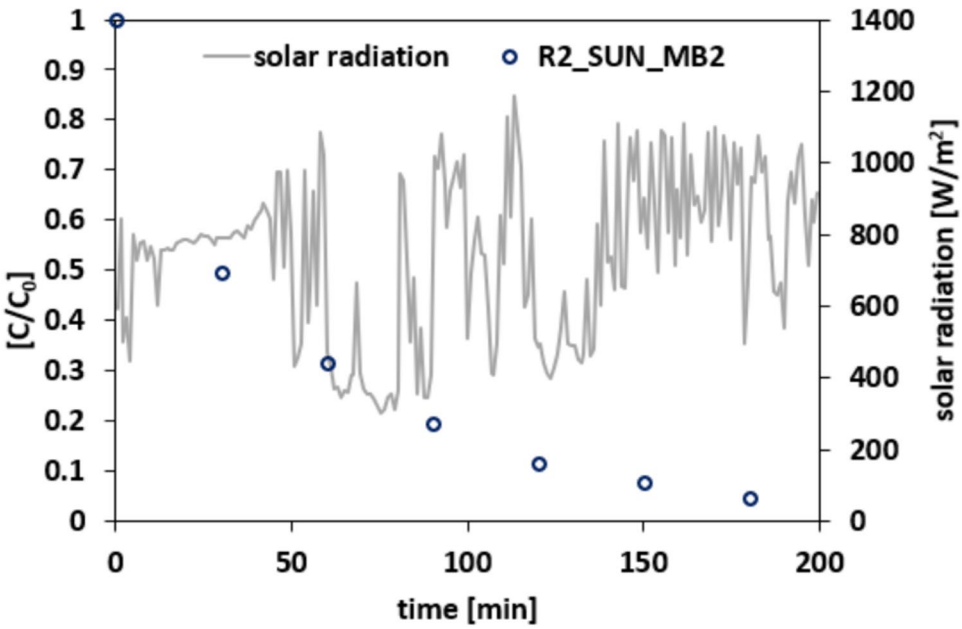

Fig. 5 Degradation of methylene blue over time under solar radiation for test R2_SUN_MB2 in the 2-profile reactor

In contrast to the outdoor test, decolorization under artificial UVA conditions in the laboratory followed a linear decay behavior and thus a zero-order reaction. After 300 min, the light transmission at 664 nm reached a rest level of approx. 29%, i.e., approx. 71% of the methylene blue was degraded within 5 h by UVA light exposure. UVA radiation represents approx. 4% of the total solar radiation, which means that it can reach a maximum value of approx. 55 W × m^{-2}. However, radiation intensity in the laboratory tests was 3.5 times higher. As decolorization in the laboratory test series significantly lagged behind outdoor test conditions, this also underlines relevance of photons of wavelength outside the UVA range, although various studies described photoactivation of titanium dioxide only in the UVA range (Banerjee et al. 2014).

Due to the differences in both degradation kinetics and reaction orders in decolorization of methylene blue, laboratory tests with artificial light solely revealed artificial test results, which did not fit to outdoor conditions.

Since the decolorization kinetics of methylene blue is nevertheless dependent on the light intensity, but the latter was not constant over the test period under outdoor

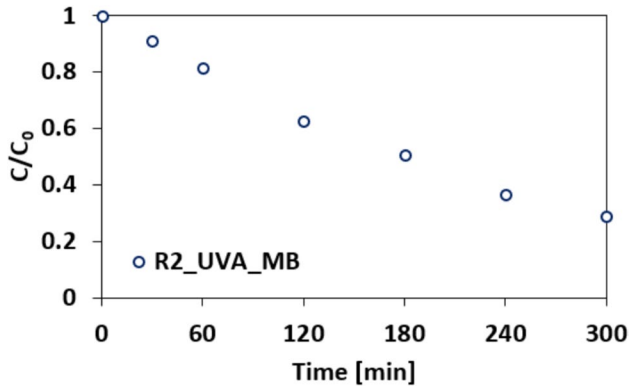

Fig. 6 Degradation of methylene blue over time under UVA light in the laboratory (test R2_UVA_MB, 385 W/m^2)

conditions, a direct comparison of the degradation kinetics under different radiation conditions is not possible. The correlation of decolorization with both time and light exposure needs reduction to a single parameter to improve comparability. This can be achieved by correlating remaining methylene blue concentrations with the global radiation intensity to derive the total light dose. Figure 7 visualized this approach. As the methylene blue concentration curves were almost identical across three test series, and therefore, independent of direct sunlight exposure, the final proof of participation of non-UVA photons in methylene blue degradation was provided. The degradation in the uncoated control reactor proved that the photocatalytic reaction was responsible for a more than doubling of the reaction rate.

The methylene blue degradation test on the R18 reactors showed similar results for the degradation kinetics. The order 1 behavior is clearly shown in Fig. 8. Since there was no recirculation in the test mode, the experiments lasted for 120 min when the solution reached the outlet of the reactor. With one through-put, after 18 profiles, the reactor was able to degrade 98.3% of the initial concentration. The decolorization effect is clearly shown in Fig. 5.

Evaluation of the disinfection potential

For the four test series with the R18 prototype, parallel tests were carried out with and without catalytic coating in order to be able to evaluate the disinfection performance attributable to the photocatalytic activity. Over the two-hour operation of the test system, clear disinfection was observed for *Pseudomonas fluorescens* (Fig. 9) in both test systems. The concentration of vegetative cells fell from 1.0×10^7 CFU × mL^{-1} over the test period to 3×10^4 CFU × mL^{-1} (uncoated system) and 8×10^2 CFU × mL^{-1} (coated system). The corresponding disinfection performance was thus 99.8% (2.7 log units) or 99.996% (4.4 log units) at a radiation intensity of 250–800 W × m^{-2} (on average 500 W × m^{-2}). Compared to the uncoated system, the cleaning performance could thus be further increased by 1.7 log levels.

In contrast, there is no catalyst-induced increase in treatment performance in *Bacillus subtilis* test series (Fig. 10). Here, both reactors show a reduction of 2.0 log units, from approx. 1.0×10^6 CFU × mL^{-1} to approx. 1.0×10^4 CFU × mL^{-1}. In addition to the different structures of the cell wall of gram-positive cells compared to gram-negative

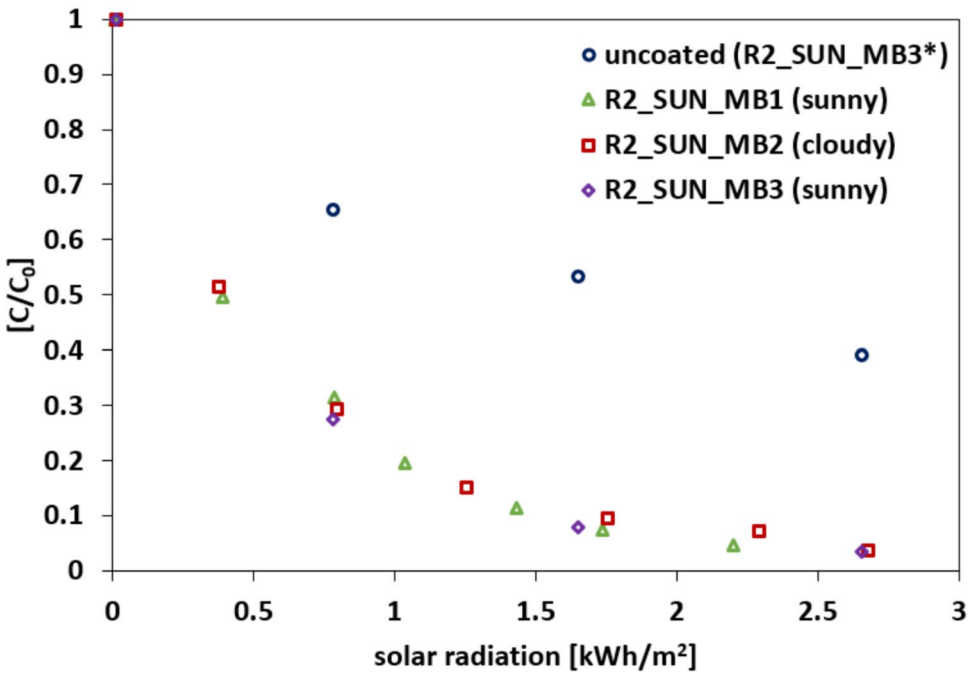

Fig. 7 2-profile reactor under sunlight and partial sunlight due to cloud cover

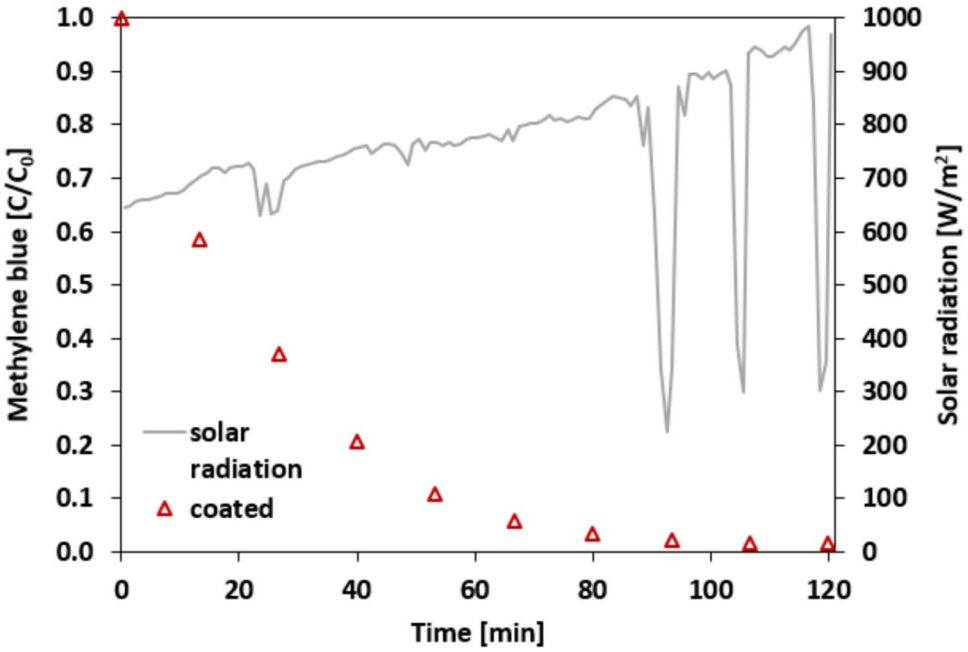

Fig. 8 Methylene blue degradation by the 18-profile reactor on a mainly sunny day

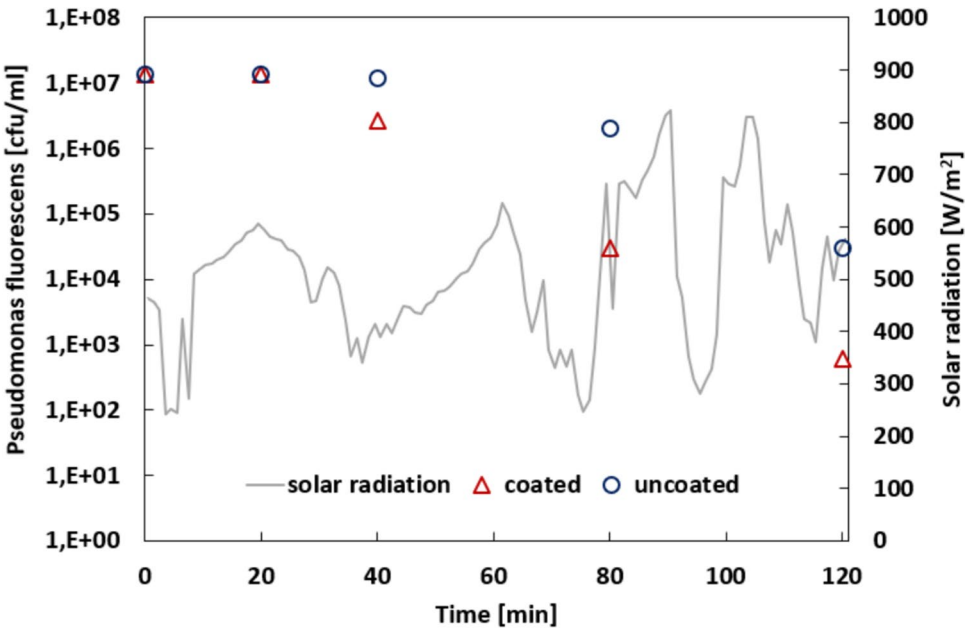

Fig. 9 Disinfection of Pseudomonas fluorescens

cells, the reason may be particularly seen in the formation of endospores. The onset of the disinfection effect within the first 40 min and the subsequent stable level of the bacterial concentration indicate that the cell wall structure is only of secondary relevance only reflected in the decay kinetics and in the comparison of the two reactor forms. The formation of stable concentration levels over time reveals the dominant effect of existing endospores, which germinated again as vegetative cells during cultivation on test media. An endospore content of approx. 1% in the liquid culture used seems to be a realistic concentration level. Differences in cell structure of endospore versus vegetative cells, and in latter case, of gram-negative versus gram-positive cells, however, cause strong effects on disinfection performance. Missing differences between coated and uncoated systems can be attributed to the increased photo-shielding of the cell wall.

Escherichia coli is generally regarded as a strain that is very easily inactivated by UV light. Masjoudi et al. (2021) described reductions of 1–5 log levels at 1.2–8.2 mJ × cm^{-2} for the E. coli strain used (*E. coli* B ATCC13033) and thus similar results as for *Pseudomonas* sp. Compared to *Bacillus subtilis* as a gram-positive strain, the UV dose is roughly a

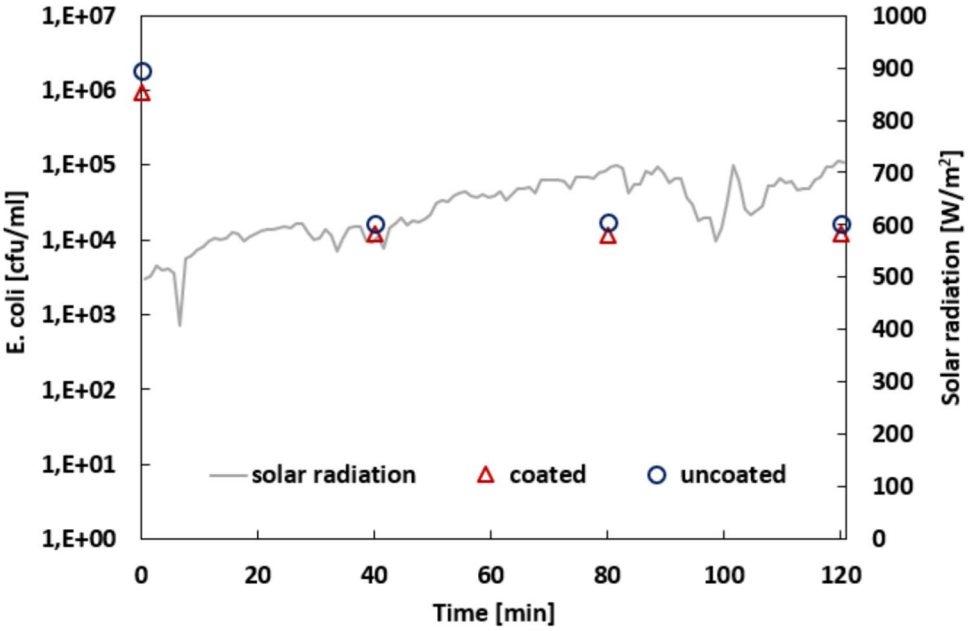

Fig. 10 Disinfection of Bacillus subtilis

factor of 10 lower (see Table 3). This correlation could not be observed in the present test series, in particular due to the lack of radiation intensity (250–600 W × m^{-2}, on average 400 W × m^{-2}). Both reactors showed no decrease in vegetative cells over the first 80 min of the test, see Fig. 11. In the last third of the test, only the uncoated reactor showed a decrease of approx. 90% or 1.0 log units. To prove that the reactor is able to degrade *E. coli*, the data for R2_SUN_Ecoli test, i.e., the performance of the 2-profile lab-scale reactor against *E. coli* and exposed to solar light, were added to the supplements. It is clearly shown that the disinfection of *E. coli* is possible with the presented reactor.

To approximate the real situation, the fourth test series was carried out with a mixed culture from the wastewater treatment plant secondary settling tank effluent. As this mixture contains a wide variety of gram-negative and gram-positive species, the cells do not appear as single dominant cells but as small flocculent agglomerates. Therefore, in contrast to laboratory cultivation, the disinfection effect is comparatively low. With sufficiently high radiation intensity (600–750 W × m^{-2}; on average 680 W/m^2), a reduction of approx. 96% or 1.4 log units could be achieved with an initial concentration of 1.1 × 10^7 CFU × mL^{-1} in the case of the uncoated reactor (Fig. 12).

Compared to UV disinfection performance with UV lamps in laboratory studies, the system understandably shows a significantly lower disinfection performance (Masjoudi et al. 2021; Hijnen 2009b). However, it must be noted that wavelengths emitted by the used UV lamps do not occur in solar radiation due to the shielding of the atmosphere and therefore cannot be tracked in a SODIS approach. The significant influence of the wavelength on the disinfection

Table 3 Reported fluences for multiple log reduction using UV light (Masjoudi et al. 2021)

Strain	Wavelength (nm)	Fluence (mJ × cm^{-2}) for logs of reduction					
		1	2	3	4	5	6
Bacillus subtilis ATCC6633	254	16–28	29–43	40–58	51–73	64–86	
Escherichia coli B ATCC13033	254	1.2	3.0	4.7	6.5	8.2	10
Pseudomonas sp.	254	1.2–2.8	2.8–5.5	4.6–7.0	6.7–9.3	No data	No data
Escherichia coli ATCC15597	297	0.5	0.7	0.9	1.1	1.4	No data
	310	191	320	360	401	442	No data
Escherichia coli CGMCC 1.3373	267	5.5	8.3	11	15	No data	No data
	275	5.6	9.3	13	No data	No data	No data
Pseudomonas aeruginosa ATCC15442	255	1.7	3.3	4.2	5.3	7.7	No data
	265	1.4	2.8	4.2	5.5	No data	No data
	285	2.0	3.7	5.0	7.0	No data	No data

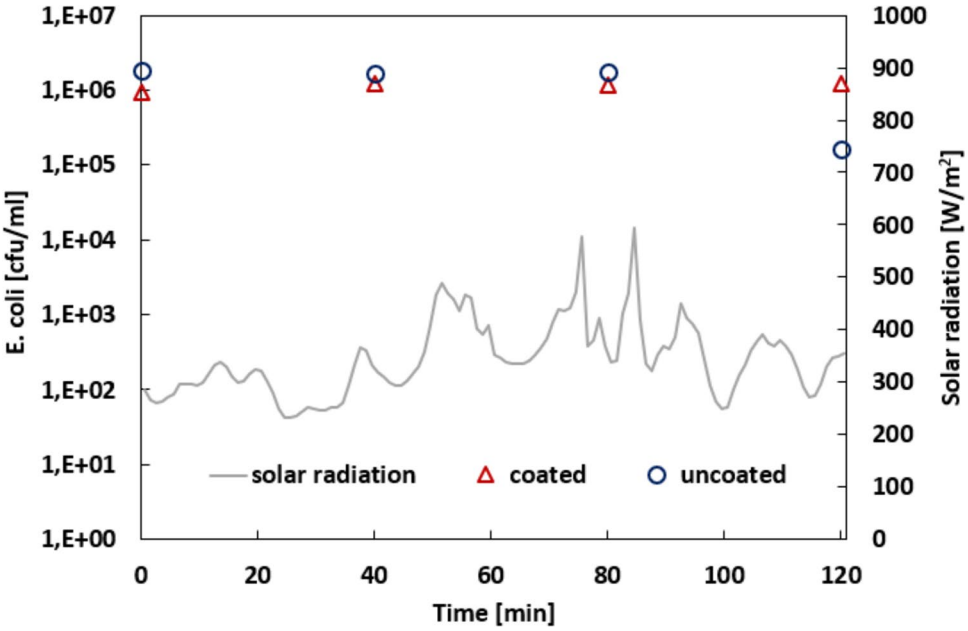

Fig. 11 Disinfection of E. coli

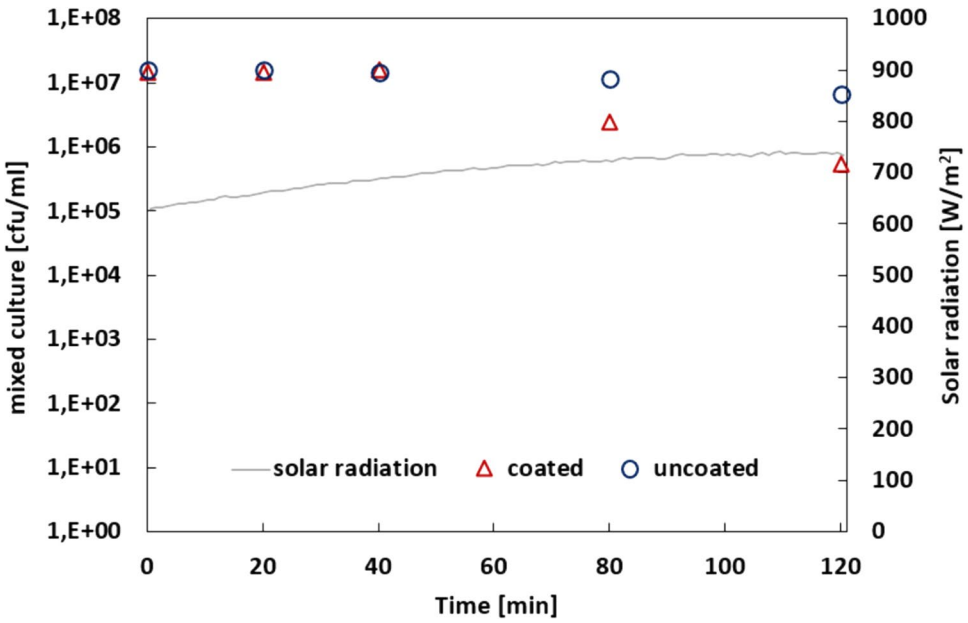

Fig. 12: Disinfection of a mixed culture

effect has already been described in several studies (both Lara de Larrea et al. 2023; Mbonimpa et al. 2018; Masjoudi et al. 2021).

Masjoudi et al (2021) described extreme differences in the UV fluence required for comparable disinfection efficiencies for parallel tests at wavelengths of 297 nm and 310 nm. The direct comparison showed that disinfection at 310 nm required fluences approx. 350 times higher than at 297 nm. De Larrea et al (2023) Klicken oder tippen Sie hier, um Text einzugeben. made a similar statement for test series with *Pseudomonas fluorescens*, where reductions by 1.0, 2.0, 3.0 and 4.0 log units required fluences of approx.. 1.5, 5.0, 8.0, 10.5 mJ × cm^{-2} at a wavelength of 280 nm, whereas at 365 nm—and thus in the UVA light range—only reductions of 1.75–2.0 log units were observed for fluences of 20–120 mJ × cm^{-2} (all data from graphical readout). These data are comparable with the data presented here with regard to the disinfection effect, although lower UV fluences were used in the present tests (500 W × m^{-2} at a share of 4% UVA correspond to 21.6 mJ × cm^{-2}).

Reactor and operation

The reactor is characterized by its simple operation and cost-effective manufacturing process. The use of aluminum U-profiles, which are widely available and inexpensive, enables straightforward construction. For the 3D-printed components, a standard 3D printer is sufficient, as it can produce parts from low-cost polylactide (PLA). The supporting structure can be made from wood or other locally available materials, offering flexibility in construction. The flow-through operation is equally simple: The water to be treated is introduced at the top and exits the reactor at the bottom in a purified state. A key advantage of this system is that it does not require professionally trained personnel for operation, making it highly accessible for decentralized applications. Additionally, the reactor contains no expensive technical components that could fail or require complex maintenance, further reducing operational costs and ensuring long-term reliability.

However, this simple and economical design also presents certain challenges. The open-profile configuration makes the reactor particularly susceptible to the entry of debris and other contaminants, which may compromise performance. Additionally, an additional filtration stage is required, as suspended solids can easily enter the system. For large-scale applications, the integration of pre- and posttreatment steps, such as sand filters, would be necessary to remove particulates before they enter the reactor and to minimize fouling after treatment. Another critical factor is the proper leveling of the reactor. If not positioned on a stable and even surface, variations in water height across the profile width may occur, leading to localized overflow and uneven flow distribution.

These aspects are crucial considerations for scaling up the system for widespread implementation and will be further refined in the future development efforts.

Conclusion

Based on the SODIS approach, a reactor concept consisting of 18 aluminum U-profiles coated with a potassium silicate-based geopolymer, known as water glass, which also contains the TiO_2 as a catalyst, was used to investigate the removal of methylene blue as chemical as well as *E. coli, Bacillus subtilis, Pseudomonas fluorescens* and a mixed culture as biological indicator contaminants under real sunlight exposure.

The cleaning efficiency against methylene blue was increased by the coating from 63 to 99% at 180 min sunlight exposure. In addition to the solar light intensity, the disinfection performance depended in particular on different physiology (including the structure of the cell wall and Gram behavior), physiological state, strain variations, the occurrence of different protective and repair mechanisms against oxidative stress and the form of cultivation (i.e., single cell, flocs, biofilm) and led to wide variations in efficiencies. The coated system was characterized by a higher efficiency with 0.0–4.4 log unit reduction compared to the uncoated system with 0.0–2.7 log units. The degradation kinetics toward methylene blue and bacterial contamination obeyed a 1 st-order reaction order. Comparing conditions of solar light exposure with artificial UVA light irradiation results indicate involvement of other solar light photons in the degradation reaction.

The presented concept is at least equal to or more efficient than literature references with UVA light irradiation in terms of dose-specific cleaning performance.

Supplementary Information The online version contains supplementary material available at https://doi.org/10.1007/s13201-025-02453-x.

Acknowledgements We would like to thank Dipl. Ing. Andreas Vogel and Willi Schwan for their technical support and the interesting discussion about the results. Furthermore, Dr. Jochen Seidel for providing the solar data of the meteorological station Lauchäcker on the university campus Stuttgart.

Funding Open Access funding enabled and organized by Projekt DEAL.

Declarations

Conflict of interest This project was funded by Boysen Stiftung (BOY-185). The funders had no role in study design, data collection and analysis, decision to publish or preparation of the manuscript. The authors have no competing interests to declare that are relevant to the content of this article.

Ethical approval The authors declare that this research was conducted under ethical guidelines and standards.

References

Adelodun B, Ajibade FO, Ighalo JO, Odey G, Ibrahim RG, Kareem KY et al (2021) Assessment of socioeconomic inequality based on virus-contaminated water usage in developing countries: a review. Environ Res 192:110309. https://doi.org/10.1016/j.envres.2020.110309

Alrousan DMA, Polo-López MI, Dunlop PSM, Fernández-Ibáñez P, Byrne JA (2012) Solar photocatalytic disinfection of water with immobilised titanium dioxide in re-circulating flow CPC reactors. Appl Catal B: Environ 128:126–134. https://doi.org/10.1016/j.apcatb.2012.07.038

Banaś AK, Zgłobicki P, Kowalska E, Dziga D, Strzałka W (2020) All you need is light. Photorepair of UV-induced pyrimidine dimers. Genes. https://doi.org/10.3390/genes11111304

Banerjee S, Pillai SC, Falaras P, O'shea KE, Byrne JA, Dionysiou DD (2014) New insights into the mechanism of visible light photocatalysis. J Phys Chem lett 5(15):2543–2554. https://doi.org/10.1021/jz501030x

Baral R, Nonvignon J, Debellut F, Agyemang SA, Clark A, Pecenka C (2020) Cost of illness for childhood diarrhea in low- and middle-income countries: a systematic review of evidence and modelled estimates. BMC Public Health 20(1):619. https://doi.org/10.1186/s12889-020-08595-8

Bojinova A, Kralchevska R, Poulios I, Dushkin C (2007) Anatase/rutile TiO2 composites: influence of the mixing ratio on the photocatalytic degradation of malachite green and orange II in slurry. Mater Chem Phys 106(2–3):187–192. https://doi.org/10.1016/j.matchemphys.2007.05.035

Botzenhart K (2007) Viren im Trinkwasser. Bundesgesundheitsblatt, Gesundheitsforschung, Gesundheitsschutz 50(3):296–301. https://doi.org/10.1007/s00103-007-0155-4

Bundesministerium für Gesundheit (2001) Verordnung über die Qualität von Wasser für den menschlichen Gebrauch - Trinkwasserverordnung. TrinkwV

Chen Chih-Yu, Wu Li-Chun, Chen Hsuan-Yu, Chung Ying-Chien (2010) Inactivation of staphylococcus aureus and *Escherichia coli* in water using photocatalysis with Fixed TiO2. Water Air Soil Pollut 212(1–4):231–238. https://doi.org/10.1007/s11270-010-0335-y

Cleaver JE (1974) Repair Processes for Photochemical Damage in Mammalian Cells. In vol. 4: Elsevier (Advances in Radiation Biology), pp 1–75

Deng Y, Li Z, Tang R, Ouyang K, Liao C, Fang Y et al (2020) What will happen when microorganisms "meet" photocatalysts and photocatalysis? Environ Sci: Nano 7(3):702–723

DIN EN 903 (1994) DIN EN 903: Wasserbeschaffenheit; Bestimmung von anionischen oberflächenaktiven Stoffen durch Messung des Methylenbau-Index MBAS. Available online at https://webstore.ansi.org/standards/din/dinen9031994de

Dionysiou DD, Bahnemann D, Puma GL, Ye J, Schneider J (eds) (2016) Photocatalysis. Applications. Royal Society of Chemistry (Great Britain). Cambridge: Royal Society of Chemistry (RSC energy and environment series, 15). Available online at https://search.ebscohost.com/login.aspx?direct=true&scope=site&db=nlebk&db=nlabk&AN=1216052

Dufner L, Aresté-Saló L, Graells M, Pérez-Moya M, Kern F, Rheiheimer W (2024) Download full issue Elsevier Open Ceramics Volume 18, June 2024, 100599 Open Ceramics Photocatalytic degradation of paracetamol on immobilized TiO2 in a low-tech reactor by solar light for water treatment. Open Ceramics (18). Available online at https://doi.org/10.1016/j.oceram.2024.100599

Dufner L, Ott F, Otto N, Lembcke T, Kern F (2023) Immobilization of TiO2 photocatalysts for water treatment in geopolymer based coatings. Catalysts 13(5):898. https://doi.org/10.3390/catal13050898

Dungumaro Esther W (2007) Socioeconomic differentials and availability of domestic water in South Africa. Phys Chem Earth, Parts A/B/C 32(15–18):1141–1147. https://doi.org/10.1016/j.pce.2007.07.006

Dunlop PSM, Sheeran CP, Byrne JA, McMahon MAS, Boyle MA, McGuigan KG (2010) Inactivation of clinically relevant pathogens by photocatalytic coatings. J Photochem Photobiol A: Chem 216(2–3):303–310. https://doi.org/10.1016/j.jphotochem.2010.07.004

Falkenmark Malin (1990) Rapid population growth and water scarcity: the predicament of tomorrow's Africa. Population Dev Rev 16:81. https://doi.org/10.2307/2808065

Fouad M, Alalm MG, El-Etriby HK, Boffito DC, Ookawara S, Ohno T, Fujii M (2021) Visible-light-driven photocatalytic disinfection of raw surface waters (300–5000 CFU/mL) using reusable coated Ru/WO3/ZrO2. J Hazard Mater 402:123514. https://doi.org/10.1016/j.jhazmat.2020.123514

Fox MA, Dulay MT (1993) Heterogeneous photocatalysis. Chem Rev 93(1):341–357. https://doi.org/10.1021/cr00017a016

García-Gil Á, García-Muñoz RA, McGuigan KG, Marugán J (2021) Solar water disinfection to produce safe drinking water: a review of parameters, enhancements, and modelling approaches to make SODIS faster and safer. Molecules (Basel, Switzerland) 1:9. https://doi.org/10.3390/molecules26113431

Guimarães JR, Barretto AS (2003) Photocatalytic inactivation of Clostridium perfringens and coliphages in water. Braz J Chem Eng 20(4):403–411. https://doi.org/10.1590/s0104-66322003000400007

Gutiérrez-Alfaro S, Acevedo A, Rodríguez J, Carpio EA, Manzano MA (2016) Solar photocatalytic water disinfection of *Escherichia coli*, *Enterococcus spp*. and clostridium perfringens using different low-cost devices. J Chem Tech Biotech 91(7):2026–2037. https://doi.org/10.1002/jctb.4795

Hasan MZ, Mehdi GG, De Broucker G, Ahmed S, Ali MW, Del Campo JM et al (2021) The economic burden of diarrhea in children under 5 years in Bangladesh. Int J Infect Dis: IJID: Off Publ Int Soc Infect Dis 107:37–46. https://doi.org/10.1016/j.ijid.2021.04.038

Herigstad B, Hamilton M, Heersink J (2001) How to optimize the drop plate method for enumerating bacteria. J Microbiol Methods 44(2):121–129. https://doi.org/10.1016/S0167-7012(00)00241-4

Hijnen WAM (2009a) Elimination of micro-organisms in water treatment. KWR Watercycle Research Institute, Nieuwegein

Hijnen WAM (2009b) Elimination of micro-organisms in water treatment. Eliminatie van micro-organismen in de waterzuivering. Doctor thesis. University of Utrecht, Utrecht

Hijnen WAM, Medema GJ (2005) Inactivation of viruses, bacteria, spores and protozoa by ultraviolet irradiation in drinking water practice: a review. Water Supply 5(5):93–99. https://doi.org/10.2166/ws.2005.0043

Hoben HJ, Somasegaran P (1982) Comparison of the pour, spread, and drop plate methods for enumeration of *Rhizobium spp*. in inoculants made from presterilized peat. Appl Environ Microbiol 44(5):1246–1247. https://doi.org/10.1128/aem.44.5.1246-1247.1982

Hunter PR (2009) Household water treatment in developing countries: comparing different intervention types using meta-regression. Environ Sci Technol 43(23):8991–8997. https://doi.org/10.1021/es9028217

Ide Y, Inami N, Hattori H, Saito K, Sohmiya M, Tsunoji N et al (2016) Remarkable charge separation and photocatalytic efficiency enhancement through interconnection of TiO2 nanoparticles by hydrothermal treatment. Angewandte Chemie (International ed. in English) 55(11):3600–3605. https://doi.org/10.1002/anie.201510000

International Astronomical Union (2015) Resolution B2 on recommended zero points for the absolute and apparent bolometric magnitude scales. Proposed by IAU Inter-Division A-G Working Group on Nominal Units for Stellar and Planetary Astronomy. Edited by International Astronomical Union. International Astronomical Union. Paris. Available online at https://www.iau.org/static/resolutions/IAU2015_English.pdf

Ismael M (2020) A review and recent advances in solar-to-hydrogen energy conversion based on photocatalytic water splitting over

doped-TiO2 nanoparticles. Sol Energy 211:522–546. https://doi.org/10.1016/j.solener.2020.09.073
Khan SJ, Reed RH, Rasul MG (2012) Thin-film fixed-bed reactor for solar photocatalytic inactivation of Aeromonas hydrophila: influence of water quality. BMC Microbiol 12:285. https://doi.org/10.1186/1471-2180-12-285
Koltsakidou A, Antonopoulou M, Evgenidou E, Konstantinou I, Giannakas AE, Papadaki M et al (2017) Photocatalytical removal of fluorouracil using TiO2-P25 and N/S doped TiO2 catalysts: a kinetic and mechanistic study. Sci Total Environ 578:257–267. https://doi.org/10.1016/j.scitotenv.2016.08.208
Kuzminov A (2013) Pyrimidine Dimers. In: Brenner's Encyclopedia of Genetics. Elsevier, pp 538–539
Landesanstalt für Umwelt Baden-Württemberg: Solare Einstrahlung. Globalstrahlung. Ministerium für Umwelt, Klima und Energiewirtschaft Baden-Württemberg. Available online at https://www.energieatlas-bw.de/sonne/dachflachen/hintergrundinformationen/solare-einstrahlung, checked on 2/6/2024
Lara de Larrea J, MacIsaac SA, Rauch KD, Stoddart AK, Gagnon GA (2023) Comparison of legionella pneumophila and pseudomonas fluorescens quantification methods for assessing UV LED disinfection. ACS ES&T Water 3(11):3667–3675. https://doi.org/10.1021/acsestwater.3c00428
Li G-Q, Wang W-L, Huo Z-Y, Lu Y, Hu H-Y (2017) Comparison of UV-LED and low pressure UV for water disinfection: Photoreactivation and dark repair of *Escherichia coli*. Water Res 126:134–143. https://doi.org/10.1016/j.watres.2017.09.030
Loeb S, Hofmann R, Kim J-H (2016) Beyond the pipeline: assessing the efficiency limits of advanced technologies for solar water disinfection. Environ Sci Technol Lett 3(3):73–80. https://doi.org/10.1021/acs.estlett.6b00023
Lonnen J, Kilvington S, Kehoe SC, Al-Touati F, McGuigan KG (2005) Solar and photocatalytic disinfection of protozoan, fungal and bacterial microbes in drinking water. Water Res 39(5):877–883. https://doi.org/10.1016/j.watres.2004.11.023
Malato S, Fernández-Ibáñez P, Maldonado MI, Blanco J, Gernjak W (2009) Decontamination and disinfection of water by solar photocatalysis: recent overview and trends. Catal Today 147(1):1–59. https://doi.org/10.1016/j.cattod.2009.06.018
Masjoudi Mahsa, Mohseni Madjid, Bolton James R (2021) Sensitivity of bacteria, protozoa, viruses, and other microorganisms to ultraviolet radiation. J Res Natl Inst Stan. https://doi.org/10.6028/jres.126.021
Mbonimpa EG, Blatchley ER, Applegate B, Harper WF (2018) Ultraviolet A and B wavelength-dependent inactivation of viruses and bacteria in the water. J Water Health 16(5):796–806. https://doi.org/10.2166/wh.2018.071
McGuigan KG, Conroy RM, Mosler HJ, du Preez M, Ubomba-Jaswa E, Fernandez-Ibanez P (2012) Solar water disinfection (SODIS): a review from bench-top to roof-top. J Hazard Mater 235–236:29–46. https://doi.org/10.1016/j.jhazmat.2012.07.053
Moreno-SanSegundo J, Giannakis S, Samoili S, Farinelli G, McGuigan KG, Pulgarín C, Marugán J (2021) SODIS potential: a novel parameter to assess the suitability of solar water disinfection worldwide. Chem Eng J 419:129889. https://doi.org/10.1016/j.cej.2021.129889
Ochiai T, Fujishima A (2012) Photoelectrochemical properties of TiO2 photocatalyst and its applications for environmental purification. J Photochem Photobiol C: Photochem Rev 13(4):247–262. https://doi.org/10.1016/j.jphotochemrev.2012.07.001
Oelgemöller M, Healy N, de Oliveira L, Jung C, Mattay J (2006) Green photochemistry: solar-chemical synthesis of Juglone with medium concentrated sunlight. Green Chem 8(9):831–834. https://doi.org/10.1039/B605906F
Omar A, Ali MS, Abd Rahim N (2020) Electron transport properties analysis of titanium dioxide dye-sensitized solar cells (TiO2-DSSCs) based natural dyes using electrochemical impedance spectroscopy concept: a review. Sol Energy 207:1088–1121. https://doi.org/10.1016/j.solener.2020.07.028
Pichat P (ed) (2013) Photocatalysis and water purification. From fundamentals to recent applications. Weinheim: Wiley-VCH-Verl. (Materials for sustainable energy and development)
Quek PH, Hu J (2008) Indicators for photoreactivation and dark repair studies following ultraviolet disinfection. J Ind Microbial Biotechnol 35(6):533–541. https://doi.org/10.1007/s10295-008-0314-0
Rahut DB, Behera B, Ali Akhter (2015) Household access to water and choice of treatment methods: empirical evidence from Bhutan. Water Resour Rural Dev 5:1–16. https://doi.org/10.1016/j.wrr.2014.09.003
Rauf MA, Meetani MA, Khaleel A, Ahmed A (2010) Photocatalytic degradation of Methylene Blue using a mixed catalyst and product analysis by LC/MS. Chem Eng J 157(2–3):373–378. https://doi.org/10.1016/j.cej.2009.11.017
Reed RW, Reed GB (1948) "Drop plate" method of counting viable bacteria. Can J Res 26(6):317–326. https://doi.org/10.1139/cjr48e-020
Schneider J, Bahnemann D, Ye J, Li Puma G, Dionysiou DD (eds) (2016) Photocatalysis. Cambridge: Royal Society of Chemistry (RSC energy and environment series, no. 14)
Shannon MA, Bohn PW, Elimelech M, Georgiadis JG, Mariñas BJ, Mayes AM (2008) Science and technology for water purification in the coming decades. Nature 452(7185):301–310. https://doi.org/10.1038/nature06599
Svoboda L, Licciardello N, Dvorský R, Bednář J, Henych J, Cuniberti G (2020) Design and performance of novel self-cleaning g-C3N4/PMMA/PUR membranes. Polymers. https://doi.org/10.3390/polym12040850
UNICEF (2012) Pneumonia and Diarrhoea: Tackling the Deadliest Diseases for the World´s Poorest Children. Edited by UNICEF Publications. UNICEF (65491). Available online at https://www.unicef.org/publications/index_65491.html
Unidted Nations (2015) The 17 Goals. Edited by Department of Economic and Social Affairs
Vasiljevic ZZ, Dojcinovic MP, Vujancevic JD, Jankovic-Castvan I, Ognjanovic M, Tadic NB et al (2020) Photocatalytic degradation of methylene blue under natural sunlight using iron titanate nanoparticles prepared by a modified sol-gel method. Roy Soc Open Sci 7(9):200708. https://doi.org/10.1098/rsos.200708
WHO (2017) Guidelines for drinking-water quality. Fourth edition incorporating the first addendum. Geneva: World Health Organization. Available online at https://www.ncbi.nlm.nih.gov/books/NBK442376/
WHO (2022a) Drinking-water. Key facts. Edited by World Health Organization. Available online at https://www.who.int/news-room/fact-sheets/detail/drinking-water
WHO (2022b) Sanitation. Key facts. Edited by World Health Organization. Available online at https://www.who.int/news-room/fact-sheets/detail/sanitation
Xia S, Zhang L, Pan G, Qian P, Ni Z (2015) Photocatalytic degradation of methylene blue with a nanocomposite system: synthesis, photocatalysis and degradation pathways. Phys Chem Chem Phys: PCCP 17(7):5345–5351. https://doi.org/10.1039/c4cp03877k